

High-pressure polymorphs of anatase TiO₂

T. Arlt

Bayerisches Geoinstitut, University of Bayreuth, D-95440 Bayreuth, Germany

M. Bermejo and M. A. Blanco

Departamento de Química Física y Analítica, Facultad de Química, Universidad de Oviedo, E-33006 Oviedo, Spain

L. Gerward* and J. Z. Jiang

Department of Physics, Building 307, Technical University of Denmark, DK-2800 Kongens Lyngby, Denmark

J. Staun Olsen

Niels Bohr Institute for Astronomy, Physics and Geophysics, Ørsted Laboratory, DK-2100 Copenhagen, Denmark

J. M. Recio

Departamento de Química Física y Analítica, Facultad de Química, Universidad de Oviedo, E-33006 Oviedo, Spain

(Received 16 November 1999)

The equation of state of anatase TiO₂ has been determined experimentally—using polycrystalline as well as single-crystal material—and compared with theoretical calculations using the *ab initio* perturbed ion model. The results are highly consistent, the zero-pressure bulk modulus being 179(2) GPa from experiment and 189 GPa from theory. Single-crystal tetragonal anatase transforms to the orthorhombic α -PbO₂ structure at about 4.5 GPa. This transition is suppressed in the polycrystalline material at room temperature, probably due to the presence of grain boundaries and other crystal defects. Polycrystalline anatase is found to transform to the monoclinic baddeleyite structure at about 13 GPa. Upon decompression, the baddeleyite phase transforms to the α -PbO₂ phase at about 7 GPa. The experimental zero-pressure bulk moduli are 258(8) GPa for the α -PbO₂ phase and 290(10) GPa for the baddeleyite phase.

I. INTRODUCTION

Titanium dioxide (TiO₂) exists in nature as the minerals rutile, anatase, and brookite. There have been many studies of the electronic and structural properties of titanium dioxide, experimental as well as theoretical. However, only the rutile phase has been studied extensively. Rutile is an important rock-forming mineral and the most abundant TiO₂ polymorph in nature. In addition, most crystal-growth techniques basically yield titanium dioxide in the rutile phase. Anatase is less dense than rutile and also found to be less stable.^{1,2} Relative to rutile there are fewer investigations of the anatase phase, although it constitutes most of the commercially produced material. Due to its high refractive index and lack of absorption of visible light, anatase is used as a white pigment for paints, plastics, and paper. Current research is investigating its photocatalytic properties and its use in optoelectronic devices.^{3,4} In a theoretical study, Dewhurst and Lowther⁵ suggest that a fluorite structure of TiO₂, as yet unidentified experimentally, could have a hardness approaching that of boron nitride. Recently, nanocrystalline TiO₂ has attracted some interest with respect to particle size effects on transformation kinetics and structural stability.^{6–8}

It is well known that titanium dioxide appears in high-pressure phases that are isostructural with columbite (orthorhombic α -PbO₂) and baddeleyite (monoclinic ZrO₂).^{1,9,10} High-pressure, high-temperature treatment of titanium dioxide yields the α -PbO₂ modification, which can be quenched to ambient conditions. At room-temperature compression,

rutile is preserved up to the pressure 12 GPa, where it transforms to the baddeleyite-type phase. In decompression, the latter phase transforms to the α -PbO₂ phase at 7 GPa.¹¹ Using x-ray diffraction, Haines and Léger¹² claim that anatase transforms to the α -PbO₂ phase, and above 10 GPa to the baddeleyite phase. Using Raman spectroscopy, Lagarec and Desgreniers¹³ have observed that single-crystal anatase transforms to the α -PbO₂ phase between 4.5 and 7 GPa. The resulting polycrystalline sample was then found to transform to the baddeleyite phase between 13 and 17 GPa.

The present work is an experimental and theoretical high-pressure structural study of TiO₂, using anatase as the starting material. Very precise unit-cell parameters of anatase have been determined by single-crystal x-ray diffraction. At the phase transition, however, the specimen breaks and cannot be further investigated. Using powder diffraction, it has been possible to study anatase as well as its high-pressure polymorphs, albeit with a lower resolution than in the single-crystal work. Due to the scatter of published data on the equation-of-state parameters of anatase, we have also investigated this polymorph theoretically using a quantum-mechanical method. As the results will show, the calculated high-pressure behavior of anatase is in very good agreement with the experimental data of the present work.

II. EXPERIMENTAL PROCEDURES

A. Single-crystal diffraction

A natural anatase crystal from Hardangervidda, Norway was used in the high-pressure single-crystal x-ray-diffraction

TABLE I. Experimental unit-cell parameters a , c , and V of single-crystal anatase. V_{Qtz} denotes unit-cell volume of quartz used as pressure standard. X1, X2, and X3 denote fragments of the same single-crystal.

Experiment	V_{Qtz} (Å ³)	P (GPa)	a (Å)	c (Å)	V (Å ³)
X3		0.0001 ^a	3.785 12(8)	9.511 85(13)	136.278 (6)
X1P1	110.728(13)	0.786(5)	3.781 79(16)	9.486 48(18)	135.675(12)
X1P2	107.487(7)	2.138(4)	3.776 49(10)	9.444 60(11)	134.698(8)
X1P3	103.795(8)	4.043(5)	3.769 75(10)	9.385 47(10)	133.377(7)
X2P4	104.521(8)	3.634(5)	3.771 3(2)	9.397 8(3)	133.660(16)
X2P5	105.461(7)	3.130(4)	3.773 09(19)	9.414 3(2)	134.024(14)
X2P6	108.961(7)	1.490(3)	3.779 17(16)	9.464 7(3)	135.176(12)

^aCrystal measured in air.

study. A $50 \times 75 \times 100 \mu\text{m}^3$ crystal fragment was loaded in a BGI-type diamond-anvil cell¹⁴ together with a ruby for rough pressure determination by the ruby-fluorescence technique¹⁵ and a quartz crystal to act as an internal pressure standard.¹⁶ A T301 stainless-steel gasket with a $250\text{-}\mu\text{m}$ hole and a 4:1 methanol-ethanol mixture as pressure-transmitting medium were used. Unit-cell parameters of both the anatase and the pressure calibrant quartz crystals were measured using a customized HUBER four-circle diffractometer operated with unmonochromatized Mo x-ray radiation. The technique of diffracted-beam crystal centering¹⁷ was employed to obtain correct setting angles. Details about the diffractometer and the centering procedure are given by Angel *et al.*¹⁶ The lattice parameters constrained to tetragonal symmetry were obtained by a vector-least-squares fit¹⁸ to the corrected reflection positions. After the high-pressure run, the diamond-anvil cell was unloaded and the breakdown product was identified in air using a Labram Raman spectrometer equipped with a He-Ne laser (wavelength 632.8 nm and power 15 mW).

B. Powder diffraction

The polycrystalline sample used in the present work is 99.6% TiO₂ anatase powder, purchased from Goodfellow Cambridge Ltd. High-pressure x-ray-diffraction spectra were recorded by the white-beam energy-dispersive method using synchrotron radiation in the 10–60-keV energy range. The diffractometer, working in the energy-dispersive mode, has been described elsewhere.¹⁹ High pressures were obtained in a Syassen-Holzappel-type diamond-anvil cell.²⁰ The sample and a small ruby chip were enclosed in a hole of diameter 0.2 mm in an Inconel gasket. A 16:3:1 methanol:ethanol:water mixture was used as the pressure-transmitting medium. The pressure was determined from the wavelength shift of the ruby fluorescence line using the nonlinear pressure scale of Mao *et al.*²¹ The Bragg angle associated with each series of diffraction spectra was deduced from a zero-pressure spectrum of NaCl with a known lattice constant.

High-temperature, high-pressure x-ray-diffraction data have also been obtained using MAX80 multi-anvil equipment. In this device, energy-dispersive x-ray-diffraction spectra can be recorded *in situ*, the slit-collimated x-ray beams entering and exiting between the anvils. The central part of the sample chamber consists of a cylindrical boron nitride container with an internal diameter of 1 mm. Half of the container is filled with the sample powder (anatase TiO₂ in our case), the other half is filled with NaCl powder for

calibration purposes. The cubic sample chamber is compressed by six anvils in a large hydraulic press. The pressure is determined from the lattice constant of NaCl using the Decker equation of state.²² Electric current can be sent through a graphite heater via two appropriate anvils. Each experimental run consists of a room-temperature compression to a selected pressure, followed by an isobaric heating to high temperature.

C. The equation of state

For each phase, the pressure-volume data can be described by the Birch²³ equation of state:

$$P/B_0 = \frac{3}{2}(x^{-7/3} - x^{-5/3})[1 + \frac{3}{4}(B'_0 - 4)(x^{-2/3} - 1)], \quad (1)$$

where $x = V/V_0$, V is the volume at pressure P , V_0 is the volume at zero pressure, and B_0 and B'_0 are the isothermal bulk modulus and its pressure derivative, both parameters being evaluated at zero pressure. Values of B_0 and B'_0 are obtained from a least-squares fit of Eq. (1) to the experimental PV data.

III. RESULTS FOR SINGLE-CRYSTAL ANATASE

Anatase has a tetragonal crystal structure with space group $I4_1/amd(141)$. The unit cell contains four TiO₂ formula units. At ambient conditions we obtain $a_0 = 3.785 12(8)$ and $c_0 = 9.511 85(13)$ Å in good agreement with literature data. From these data the density of mass is calculated to $\rho_0 = 3.8941(2)$ g/cm³. Thus, anatase is 8% less dense than rutile at ambient pressure.

Anatase was found to undergo a phase transition between 4 and 5 GPa (about 4.5 GPa) where the single crystal broke into a fine-grained powder. The breakdown reaction was repeated twice to confirm its reproducibility. Identification of the powder was done by Raman spectroscopy and showed the formation of the α -PbO₂ structure. The observed bands (the strongest ones at 153, 174, 288, 316, 342, 359, and 426 cm⁻¹) are in good agreement with those reported by Liu and Mernagh.¹⁰

The pressure variation of the unit-cell parameters is shown in Table I. The pressure has been determined from the quartz unit-cell volume, also given in Table I, using the equation-of-state parameters of Angel *et al.*¹⁶ The zero-pressure bulk modulus and its pressure derivative were determined by a fully weighted least-squares fit of the equation of state (1) to the PV data set. This gives $B_0 = 179(2)$ GPa

TABLE II. Experimental results for single-crystal anatase. The uncertainties in parentheses are the standard deviations in units of the last decimal place.

Lattice constant, a_0	3.785 12(8) Å
Lattice constant, c_0	9.511 85(13) Å
Unit-cell volume, V_0	136.278(6) Å ³
Density of mass, ρ_0	3.894 1(2) g/cm ³
Bulk modulus, B_0	179(2) GPa
Pressure derivative, B'_0	4.5(10)
Linear compressibility, β_a	0.001 00(2) GPa ⁻¹
Linear compressibility, β_c	0.003 30(2) GPa ⁻¹

and $B'_0=4.5(10)$ with $V_0=136.277(5)$ Å³ [the temperature is $T=298(1)$ K]. The linear compressibility β along the a and c axes of the tetragonal unit cell has been calculated from the polynomial equations

$$g_i(P) = g_i(0)(1 - \beta_i P + \delta_i P^2), \quad i = a \text{ and } c, \quad (2)$$

where $g_i(P)$ is the lattice parameter in the i -axis direction at pressure P , and δ_i is a constant that gives the pressure dependence of the compressibility. A least-squares fit gives $\beta_a=0.001 00(2)$ and $\beta_c=0.003 30(2)$ GPa⁻¹. Thus, the c axis is more compressible than the a axis. Table II summarizes the experimental results for single-crystal anatase.

IV. RESULTS FOR POLYCRYSTALLINE ANATASE

A. The anatase phase

Figure 1 shows a zero-pressure diffraction spectrum of anatase. Trace of the strongest 110 peak of rutile is visible in the spectrum. An analysis, based on peak height, indicates that the titanium dioxide sample contains approximately 1.5% rutile. The Bragg peak positions, converted to interplanar spacings d , are shown in Fig. 2 as functions of energy. Two independent runs gave practically the same parameters of the Birch equation (1). As a final result we quote B_0

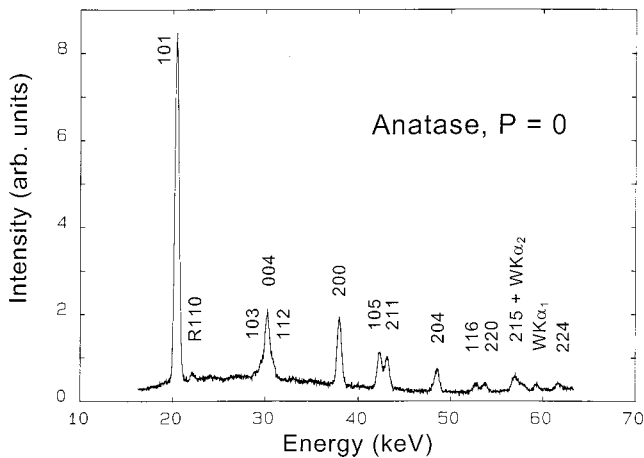


FIG. 1. Energy-dispersive powder-diffraction spectrum of TiO₂ at ambient pressure. Miller indices for the Bragg peaks are indicated. The Bragg angle is $\theta=4.95^\circ$. Intensities are given in arbitrary units. The peak denoted R110 is due to a small amount of rutile in the sample.

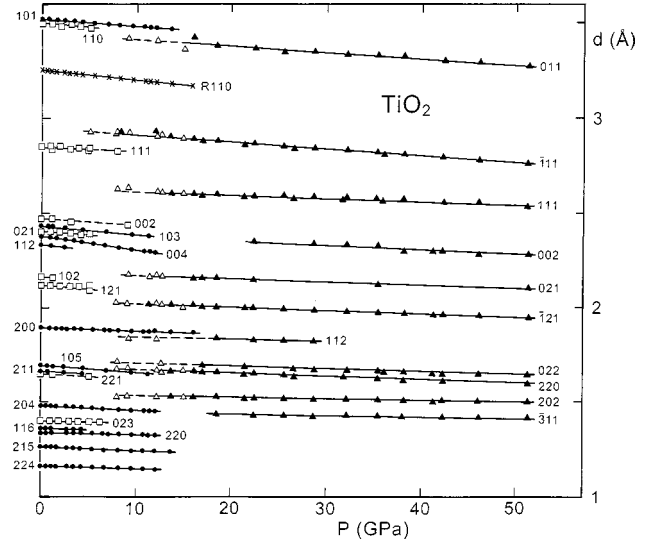


FIG. 2. Lattice plane spacing, d , obtained from powder diffraction, as a function of pressure, P . Circles denote anatase, triangles the baddeleyite phase, and squares the α -PbO₂ phase. Filled symbols and full lines denote data obtained in a compression run, open symbols and broken lines denote decompression.

$=190(10)$ GPa and $B'_0=5.3(10)$, where the uncertainty given in parentheses is the standard error in units of the last decimal place.

In contrast to the single-crystal studies, we do not observe any pressure-induced transformation of anatase to the α -PbO₂-type phase at about 4.5 GPa. The sample is found to be pure anatase until it transforms to the baddeleyite structure at about 13 GPa. Figure 3 shows the pressure-volume data for all the TiO₂ polymorphs of the present powder-diffraction study.

B. The baddeleyite phase

The baddeleyite structure has a monoclinic unit cell and space group $P2_1/c(14)$. The unit cell contains four TiO₂ formula units. By extrapolation we obtain the following zero-pressure lattice constants: $a_0=4.662(15)$, $b_0=4.969(15)$, and $c_0=4.911(15)$ Å, and $\beta_0=99.4(1)^\circ$, from which the density of mass $\rho_0=4.73(4)$ g cm⁻³ is calculated. Baddeleyite-type TiO₂ is thus 11% denser than rutile at ambient pressure. The extrapolated zero-pressure volume has been used when fitting the equation of state (1) to the baddeleyite-type PV data. Because of the uncertainty involved in the extrapolation procedure and the scatter of the PV data at the highest pressures, we have assumed that the pressure derivative of the bulk modulus is $B'_0=4.00$. The zero-pressure bulk modulus is then $B_0=290(10)$ GPa.

C. The α -PbO₂ phase

Upon decompression, the baddeleyite-type phase transforms to the orthorhombic α -PbO₂-type phase at about 7 GPa. The latter phase is the only one present after complete pressure release. This is in agreement with our previous observations with rutile as the starting material.¹¹

The α -PbO₂ type structure has an orthorhombic unit cell and space group $Pbcn(60)$. The unit cell contains four TiO₂

TABLE III. Results of aiPI+uCHF calculations for anatase TiO₂. The lattice parameters a and c have been optimized. The relative z position of oxygen in the unit cell has been fixed at the experimental value $z=0.2066$.³⁰ The calculated zero-pressure values of the lattice constants; the bulk modulus and its pressure derivative; and the linear compressibilities are $V_{0,\text{calc}}=143.8 \text{ \AA}^3$, $a_{0,\text{calc}}=3.780 \text{ \AA}$, and $c_{0,\text{calc}}=10.05 \text{ \AA}$, $B_0=189.5 \text{ GPa}$ and $B'_0=3.4$; and $\beta_{a,\text{calc}}=0.00162 \text{ GPa}^{-1}$ and $\beta_{c,\text{calc}}=0.00185 \text{ GPa}^{-1}$.

P (GPa)	V/V_0	a/a_0	c/c_0
0.0938	0.999 51	1.000 00	1.000 00
2.0959	0.989 20	0.996 71	0.996 23
4.1915	0.978 90	0.993 40	0.992 44
6.3851	0.968 59	0.990 05	0.988 65
8.6813	0.958 29	0.986 67	0.984 84
11.0852	0.947 98	0.983 25	0.981 04
13.6020	0.937 68	0.979 80	0.977 23
16.2373	0.927 38	0.976 32	0.973 40
18.9970	0.917 07	0.972 80	0.969 56
21.8873	0.906 77	0.969 24	0.965 71
24.9148	0.896 46	0.965 65	0.961 85
28.0864	0.886 16	0.962 03	0.957 97
34.8920	0.865 55	0.954 66	0.950 19
42.3688	0.844 94	0.947 14	0.942 35
50.5894	0.824 33	0.939 47	0.934 45

molecules. At ambient pressure we obtain the lattice constants $a_0=4.541(6)$, $b_0=5.493(8)$, and $c_0=4.906(9) \text{ \AA}$ in good agreement with literature data.²⁴ The calculated zero-pressure density is $\rho_0=4.336(12) \text{ g cm}^{-3}$. Thus, the α -PbO₂-type phase is 2% denser than rutile at ambient pressure.

In a high-pressure, high-temperature experiment, the α -PbO₂-type phase was quenched from 6.65 GPa and 900 °C. The equation of state was then determined from a room temperature, isothermal compression to 10 GPa. By fitting the equation of state (1) to the observed PV data, we obtain $B_0=258(8) \text{ GPa}$ and $B'_0=4.1(3)$. Subsequently, we have learned that our results are in very good agreement with Akaogi *et al.*,²⁵ who have found $B_0=253(4) \text{ GPa}$, assuming $B'_0=4.00$.

V. THEORETICAL CALCULATIONS

We have followed a quantum-mechanical approach to describe theoretically the equation of state (EOS) of the anatase phase. Our theoretical method is the *ab initio* perturbed ion model (aiPI).²⁶ Briefly, we solve the Hartree-Fock (HF) equations of the TiO₂ anatase structure by breaking the crystal wave function into localized Ti⁴⁺ and O²⁻ ionic group functions. A detailed description of the computational implementation and its latest update has been given by Blanco *et al.*²⁷ For the Ti⁴⁺ and O²⁻ ions, we have used the nearly HF exponential Clementi and Roetti²⁸ basis sets. Besides, a correlation energy correction is added to the total energy using the Coulomb-Hartree-Fock method of Clementi.²⁹

Our computational strategy is as follows. First, we calculate the total energy of the anatase phase in a set of volumes that covers a range from $0.74V_e$ to $1.17V_e$, where V_e is the

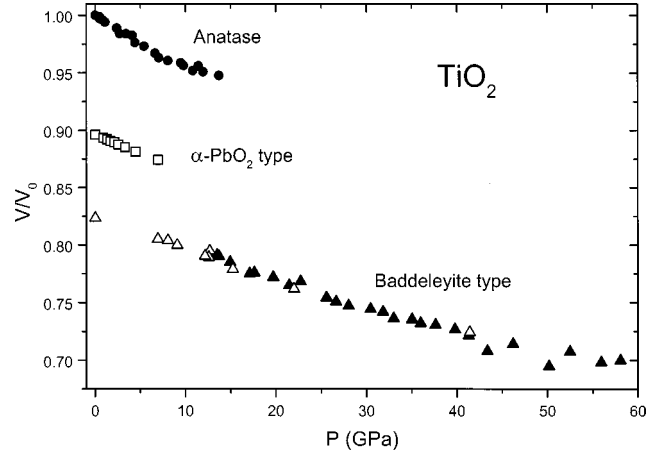


FIG. 3. Experimental pressure-volume data for the polycrystalline TiO₂ polymorphs investigated in the present work. The notation is the same as in Fig. 2. The unit-cell volumes have been normalized by dividing with $V_{0,\text{anatase}}$.

experimental unit-cell volume at normal conditions ($V_e = 136.3 \text{ \AA}^3$, cf. Table II). Second, for each volume we obtain the optimum values of the lattice parameters a and c that minimize the crystal energy, E_{crys} , whereas the oxygen parameter z is fixed to the experimental value ($z=0.2066$).³⁰ Finally, the computed (E_{crys}, V) pairs are used to calculate the pressure-volume data by minimizing the static Gibbs energy ($G = E_{\text{crys}} + PV$) with respect to V at selected values of P in the range 0–50 GPa.

We have also generated values of the zero-pressure bulk modulus and its pressure derivatives: B_0 , B'_0 , and B''_0 , by means of a numerical fitting procedure³¹ consistent with the Birch equation of state (1). Our values are 189.5 GPa, 3.42, and -0.0217 GPa^{-1} , respectively. The calculated equilibrium zero-pressure values of the unit-cell volume and the lattice constants are $V_{0,\text{calc}}=143.8 \text{ \AA}^3$, $a_{0,\text{calc}}=3.78 \text{ \AA}$, and $c_{0,\text{calc}}=10.05 \text{ \AA}$. The calculated linear compressibilities are $\beta_{a,\text{calc}}=0.00162$ and $\beta_{c,\text{calc}}=0.00185 \text{ GPa}^{-1}$. Table III summarizes the theoretical results for the anatase phase.

VI. DISCUSSION

The transformation of anatase single crystals to the α -PbO₂ structure at about 4.5 GPa is in agreement with earlier single-crystal Raman spectroscopy studies.^{10,13} However, the transformation pressure seems to be largely dependent on the specific design of the experiment and the sample used. Liu and Mernagh¹⁰ reported the irreversible transformation at 5.4(2) GPa, and Lagarec and Desgreniers¹³ between 4.5 and 7 GPa. Extrapolating the PT reaction boundaries of Dachille *et al.*¹ yields a transformation pressure of about 2.3 GPa, which indicates a considerable enhancement of the observed transition pressure at room temperature. The metastable behavior of anatase is even more pronounced in our powder data. We believe that lattice defects, in particular grain boundaries, are responsible for the missing transition to the α -PbO₂ phase in our room-temperature compression of polycrystalline anatase. In a study comparable to ours, Haines and Léger¹² describe the transition as sluggish. Moreover, they do not give any quantitative data for the transition

TABLE IV. Experimental bulk moduli of the TiO₂ polymorphs.

Polymorph	B_0 (GPa)	B'_0	ρ_0 (g/cm ³)	$\rho_0 / \rho_{0,\text{rutile}}$
Anatase	179(2)	4.5(10)	3.8941(2)	0.9166(1)
Rutile ^a	211(10)	6.5(7)	4.2485(2)	1.0000
α -PbO ₂ type	258(8)	4.1(3)	4.336(12)	1.021(1)
Baddeleyite type	290(10)	4.0 ^b	4.728(15) ^c	1.113(1)

^aData from Gerward and Olsen (Ref. 11).

^bAssumed value.

^cExtrapolated value.

pressure of the claimed anatase to α -PbO₂ phase transformation.

The phase transition from anatase to the α -PbO₂-type phase seems to have been most clearly seen in the single-crystal Raman-scattering studies by Lagarec and Desgreniers.¹³ It is reasonable to assume that polycrystalline samples contain more lattice defects than single-crystal anatase, in particular grain boundaries, which may prevent the transition at room temperature. It should be noted, however, that we do observe the transition from anatase to the α -PbO₂ phase by applying a moderate heating at high pressure. Thus, we have found that the α -PbO₂ phase appears between 200 and 400 °C in a sample compressed to 4.5 GPa.

Table IV summarizes our experimental data on the equation-of-state parameters of the TiO₂ polymorphs. For completeness, also data for rutile are included. There is a considerable scatter in the literature about the zero-pressure value of the bulk modulus of anatase. Haines and Léger¹² have reported a very low value of 59 GPa. Also their corresponding B_0 values for the α -PbO₂ (98 GPa) and baddeleyite (522 GPa) phases are in disagreement with our results. The very large B_0 value (360 GPa) for anatase, reported by Lagarec and Desgreniers,¹³ should be considered with some caution, because it has been obtained from three experimental points only. On the theoretical side, Mo and Ching³² have got 272 GPa, and Dewhurst and Lowther⁵ 194 GPa for anatase. In the present work, we obtain 179(2) GPa from experiment and 189 GPa from theory. Thus, there is a good agreement between theory and experiment in the present work.

We observe that the aiPI model tends to overestimate the unit-cell volume, $V_{0,\text{calc}}$, by about 5% compared with the experimental value. This is mainly due to a corresponding overestimation of the lattice constant along the c axis, whereas $a_{0,\text{calc}}$ is close to the experimental value. The calculated linear compressibility $\beta_{c,\text{calc}}$ is larger than $\beta_{a,\text{calc}}$ in agreement with experiment, but the difference is smaller than observed experimentally (cf. Sec. III). We relate these discrepancies to a limitation of the aiPI model, which considers only spherical distortions for the electronic density of the ions.

Mo and Ching³² have found that the zero-pressure bulk modulus of anatase is larger than that of rutile. Whereas we agree with them in the case of their B_0 value for rutile, their corresponding value for anatase is more than 70 GPa larger than our experimental and theoretical values. In contrast, the most recent theoretical B_0 value for anatase, calculated by Dewhurst and Lowther,⁵ is close to our experimental and theoretical results. The Dewhurst and Lowther B_0 value of anatase is 20% lower than that of rutile, whereas our experi-

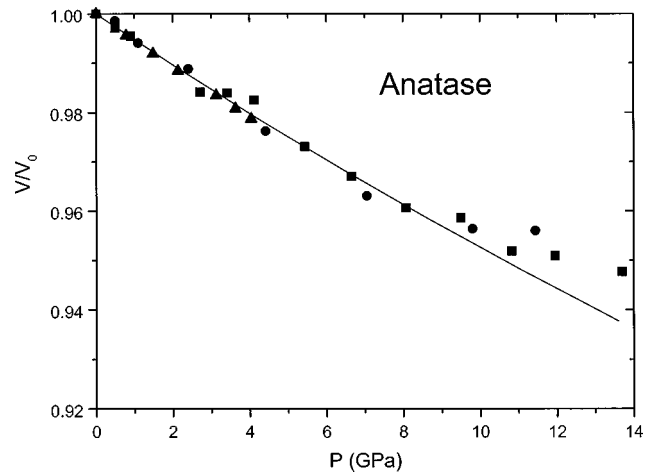


FIG. 4. Relative volume of anatase TiO₂. Circles and squares denote two experimental runs with polycrystalline anatase, triangles denote single-crystal data, and the solid curve is the result of the theoretical calculation using the *ab initio* perturbed ion model.

ments indicate that the anatase B_0 value should be about 10% lower than that of rutile. We have checked this issue further by computing the zero-pressure bulk modulus of rutile with our aiPI model. Following a similar computational procedure as outlined above for anatase, we obtain $B_{0,\text{rutile}} = 212$ GPa. This value is in very good agreement with experimental results, obtained by us and others, whereas Dewhurst and Lowther⁵ have obtained the somewhat larger value, $B_{0,\text{rutile}} = 243$ GPa.

As shown in Table IV, our zero-pressure bulk moduli for the TiO₂ polymorphs follow the expected sequence. First, they are all of the order of 200 GPa, a value that is basically controlled by the oxygen anion sublattice. In rutile and anatase, the oxygen positions can be derived from a cubic close-packed array. Therefore, these two polymorphs should have similar B_0 values. Second, it is seen that B_0 increases with increasing density of the polymorphs, i.e., in the order from anatase, rutile, α -PbO₂ phase, to the baddeleyite phase. Dewhurst and Lowther,⁵ in their theoretical calculations, find that the bulk moduli increase in the same order, albeit in a more narrow range than in the present work. This general trend, which is reasonable for a given material exhibiting polymorphism, gives consistency to our results. The physical reason is that the instantaneous bulk modulus B increases with pressure, and increasing density may be considered here as analogous to increasing pressure.

In Fig. 4 we show the relative volume of anatase TiO₂ as a function of pressure. For pressures below 8 GPa, the experimental points—for polycrystalline as well as single-crystal material—agree very well with the theoretical calculation (the full curve). Thus there is a highly satisfying consistency in the results of the present work. For pressures in the 9–14-GPa range, the experimental points for the polycrystalline material tend to deviate upwards in the PV diagram from the calculated equation of state. We have observed the same apparent lattice hardening for rutile.¹¹ It may be an effect of deviations from hydrostatic conditions for pressures above about 10 GPa.

ACKNOWLEDGMENTS

We thank HASYLAB-DESY for permission to use the synchrotron radiation facility. We are grateful for financial

support from the Danish Natural Sciences Research Council and the Danish Technical Research Council (J.Z.J., L.G., and J.S.O.), as well as from the Spanish DGICYT, Project No. PB96-0559 (M.B., M.A.B., and J.M.R.). We also wish to

thank F. Porsch and J. Truckenbrodt, HASYLAB station heads, for helpful assistance. R. J. Angel is thanked for his help in the high-pressure crystallography laboratory of the Bayerisches Geoinstitut.

*Corresponding author. Electronic address:

gerward@fysik.dtu.dk

- ¹F. Dacheville, P. Y. Simons, and R. Roy, *Am. Mineral.* **53**, 1929 (1968).
- ²A. Fahmiand and C. Minot, *Phys. Rev. B* **47**, 11 717 (1993).
- ³D. V. Ollis, E. Pelizzetti, and N. Serpone, in *Photocatalysis, Fundamentals and Applications*, edited by N. Serpone and E. Pelizzetti (Wiley, New York, 1989), p. 603.
- ⁴H. Tang, K. Prasad, R. Sanjinès, P. E. Schmid, and F. Lévy, *J. Appl. Phys.* **75**, 2042 (1994).
- ⁵J. K. Dewhurst and J. E. Lowther, *Phys. Rev. B* **54**, R3673 (1996).
- ⁶A. A. Gribb and J. F. Banfield, *Am. Mineral.* **82**, 717 (1997).
- ⁷R. L. Penn and J. F. Banfield, *Am. Mineral.* **83**, 1077 (1998).
- ⁸J. S. Olsen, L. Gerward, and J. Z. Jiang, *J. Phys. Chem. Solids* **60**, 229 (1999).
- ⁹B. Gou, Z. Liu, Q. Cui, H. Yang, Y. Zhao, and G. Zou, *High Press. Res.* **1**, 185 (1989).
- ¹⁰L. G. Liu and T. P. Mernagh, *Eur. J. Mineral.* **4**, 45 (1992).
- ¹¹L. Gerward and J. S. Olsen, *J. Appl. Crystallogr.* **30**, 259 (1997).
- ¹²J. Haines and J. M. Léger, *Physica B* **192**, 233 (1993).
- ¹³K. Lagarec and S. Desgreniers, *Solid State Commun.* **94**, 519 (1995).
- ¹⁴D. R. Allan, R. Miletich, and R. J. Angel, *Rev. Sci. Instrum.* **67**, 840 (1996).
- ¹⁵H. K. Mao, J. Xu, and P. M. Bell, *J. Geophys. Res., [Oceans]* **91**, 4673 (1986).
- ¹⁶R. J. Angel, D. R. Allan, R. Miletich, and L. W. Finger, *J. Appl. Crystallogr.* **30**, 461 (1997).
- ¹⁷H. E. King and L. W. Finger, *J. Appl. Crystallogr.* **12**, 374 (1979).
- ¹⁸R. L. Ralph and L. W. Finger, *J. Appl. Crystallogr.* **15**, 537 (1982).
- ¹⁹J. S. Olsen, *Rev. Sci. Instrum.* **83**, 1058 (1992).
- ²⁰G. Huber, K. Syassen, and W. B. Holzapfel, *Phys. Rev. B* **15**, 5123 (1977).
- ²¹H. K. Mao, P. M. Bell, J. W. Shaner, and D. J. Steinberg, *J. Appl. Phys.* **49**, 3276 (1978).
- ²²D. L. Decker, *J. Appl. Phys.* **42**, 3239 (1971).
- ²³F. J. Birch, *Appl. Phys.* **9**, 279 (1938); *Phys. Rev.* **71**, 809 (1947).
- ²⁴J. C. Jamieson and B. Olinger, *Science* **161**, 893 (1968).
- ²⁵M. Akaogi, K. Kusaba, J. Susaki, T. Yagi, M. Matsui, T. Kikegawa, H. Yusa, and E. Ito, in *High-Pressure Research: Application to Earth and Planetary Sciences*, edited by Y. Syono and M. H. Manghnani (Terra Scientific, Tokyo/American Geophysical Union, Washington, D.C., 1992), pp. 447–455.
- ²⁶V. Luaña and L. Pueyo, *Phys. Rev. B* **41**, 3800 (1990).
- ²⁷M. A. Blanco, V. Luaña, and A. Martín Pendás, *Comput. Phys. Commun.* **103**, 287 (1997).
- ²⁸E. Clementi and C. Roetti, *At. Data Nucl. Data Tables* **14**, 177 (1974).
- ²⁹J. Chakravorty and E. Clementi, *Phys. Rev. A* **39**, 2290 (1989), and references therein.
- ³⁰D. T. Cromer and K. Herrington, *J. Am. Chem. Soc.* **77**, 4708 (1955).
- ³¹M. A. Blanco, A. M. Pendás, E. Francisco, J. M. Recio, and R. Franco, *J. Mol. Struct.: THEOCHEM* **368**, 245 (1996).
- ³²S.-D. Mo and W. Y. Ching, *Phys. Rev. B* **51**, 13 023 (1995).